Cdc7-mediated phosphorylation of Cse4 regulates high-fidelity chromosome segregation in budding yeast

Prashant K. Mishra[a], Henry Wood[b,†], John Stanton[c,†], Wei-Chun Au[a], Jessica R. Eisenstatt[a], Lars Boeckmann[a,‡], Robert A. Sclafani[d], Michael Weinreich[e], Kerry S. Bloom[c], Peter H. Thorpe[b], and Munira A. Basrai[a,*]

[a]Genetics Branch, National Cancer Institute, National Institutes of Health, Bethesda, MD 20892; [b]Queen Mary University of London, London E1 4NS, UK; [c]University of North Carolina, Chapel Hill, NC 27599; [d]University of Colorado School of Medicine, Aurora, CO 80045; [e]Van Andel Research Institute, Grand Rapids, MI 49503

ABSTRACT **Faithful chromosome segregation maintains chromosomal stability as errors in this process contribute to chromosomal instability (CIN), which has been observed in many diseases including cancer. Epigenetic regulation of kinetochore proteins such as Cse4 (CENP-A in humans) plays a critical role in high-fidelity chromosome segregation. Here we show that Cse4 is a substrate of evolutionarily conserved Cdc7 kinase, and that Cdc7-mediated phosphorylation of Cse4 prevents CIN. We determined that Cdc7 phosphorylates Cse4 in vitro and interacts with Cse4 in vivo in a cell cycle-dependent manner. Cdc7 is required for kinetochore integrity as reduced levels of *CEN*-associated Cse4, a faster exchange of Cse4 at the metaphase kinetochores, and defects in chromosome segregation, are observed in a *cdc7-7* strain. Phosphorylation of Cse4 by Cdc7 is important for cell survival as constitutive association of a kinase-dead variant of Cdc7 (*cdc7-kd*) with Cse4 at the kinetochore leads to growth defects. Moreover, phospho-deficient mutations of Cse4 for consensus Cdc7 target sites contribute to CIN phenotype. In summary, our results have defined a role for Cdc7-mediated phosphorylation of Cse4 in faithful chromosome segregation.**

Monitoring Editor
Jorge Torres
University of California, Los Angeles

Received: Jun 22, 2021
Revised: Aug 11, 2021
Accepted: Aug 18, 2021

INTRODUCTION

Accurate chromosome segregation is essential for cell survival as errors in this process result in chromosomal instability (CIN), a phenotype that has been associated with a range of human diseases including cancer (Santaguida and Amon, 2015; Singh and Gerton, 2015). The kinetochore, composed of centromeric (*CEN*) DNA, associated proteins, and a distinct chromatin architecture, is the key regulator of high-fidelity chromosome segregation (Verdaasdonk and Bloom, 2011; Burrack and Berman, 2012; Musacchio and Desai, 2017). *CEN* DNAs in budding yeast are small in size comprised of ~125 bp of unique sequences (Clarke and Carbon, 1980), whereas *CEN* DNAs in other organisms are several mega-bases in size containing repeated sequences, satellite DNA arrays, or retrotransposon-derived DNA sequences (Verdaasdonk and Bloom, 2011; Burrack and Berman, 2012; Musacchio and Desai, 2017). Despite the variations in nucleotide composition and the size of *CEN* DNAs, the identity of *CEN* in eukaryotic organisms is defined epigenetically by specialized nucleosomes containing *CEN*-specific histone H3 variant, Cse4 (CENP-A in humans, Cid in flies, Cnp1 in fission yeast) (Sullivan *et al.*, 1994; Stoler *et al.*, 1995; Meluh *et al.*, 1998; Henikoff *et al.*, 2000; Takahashi *et al.*, 2000).

Identification of epigenetic mechanisms regulating Cse4 function has been an area of active research. Previous studies have identified several post-translational modifications of Cse4,

This article was published online ahead of print in MBoC in Press (http://www.molbiolcell.org/cgi/doi/10.1091/mbc.E21-06-0323).

†These authors contributed equally to this work.

‡Present address: University Medical Center, Rostock, Germany.

*Address correspondence to: Munira A. Basrai (basraim@nih.gov).

Abbreviations used: Cdk, cyclin-dependent kinase; *CEN*, centromere; CF, chromosome fragment; ChIP, chromatin immunoprecipitation; CIN, chromosomal instability; DDK, Dbf4-dependent kinase; FACS, fluorescence activated cell sorting; FOA, fluoro-orotic acid; FRAP, fluorescence recovery after photobleaching; GBP, GFP-binding protein; GFP, green fluorescent protein; HFD, histone fold domain; HU, hydroxyurea; IP, immunoprecipitation; LGR, log growth ratio; qPCR, quantitative PCR; RFP, red fluorescent protein; RT-qPCR, reverse transcription quantitative PCR; SPA, selective ploidy ablation; SPI, synthetic physical interaction; YPD, yeast peptone dextrose.

such as phosphorylation, ubiquitination, sumoylation, methylation, proline isomerization, and acetylation (Hewawasam *et al.*, 2010; Ranjitkar *et al.*, 2010; Samel *et al.*, 2012; Au *et al.*, 2013; Boeckmann *et al.*, 2013; Ohkuni *et al.*, 2014; Ohkuni *et al.*, 2016; Ciftci-Yilmaz *et al.*, 2018; Hoffmann *et al.*, 2018; Ohkuni *et al.*, 2018; Mishra *et al.*, 2019; Au *et al.*, 2020; Eisenstatt *et al.*, 2020; Ohkuni *et al.*, 2020; Eisenstatt *et al.*, 2021), which regulate faithful chromosome segregation. We previously identified two kinases, Ipl1 (Aurora B kinase in humans) and Cdc5 (Plk1 in humans), that phosphorylate Cse4 to prevent CIN (Boeckmann *et al.*, 2013; Mishra and Basrai, 2019; Mishra *et al.*, 2019). Ipl1-mediated phosphorylation of Cse4 regulates kinetochore–microtubule interactions and chromosome biorientation (Boeckmann *et al.*, 2013; Mishra and Basrai, 2019), whereas Cdc5-mediated mitotic phosphorylation of Cse4 contributes to high-fidelity chromosome segregation (Mishra and Basrai, 2019; Mishra *et al.*, 2019). Phosphomutants for Cse4 in consensus Ipl1 and Cdc5 sites exhibit CIN phenotype only when combined with other mutants (Boeckmann *et al.*, 2013; Mishra and Basrai, 2019; Mishra *et al.*, 2019), suggesting the role of other kinases in Cse4 phosphorylation.

In this study, we investigated a potential role for Dbf4-dependent kinase (DDK) in the phosphorylation of Cse4. The rationale for this is based on previous studies which have shown that Cdc7 associates with *CEN* chromatin, and this regulates *CEN* DNA replication initiation (Natsume *et al.*, 2013). The DDK, composed of the Cdc7 kinase and the regulatory subunit Dbf4, is essential for the initiation of DNA replication modulated by phosphorylation of Cdc45 and subunits of the mini-chromosome maintenance complex (Mcm2-7) (Lei *et al.*, 1997; Owens *et al.*, 1997; Weinreich and Stillman, 1999; Zou and Stillman, 2000; Bruck and Kaplan, 2009). Mutation in *MCM5* (*mcm5-bob1*) bypasses the requirement of Cdc7 for replication initiation and leads to suppression of temperature sensitivity and DNA replication defects in a *cdc7-7* strain (Hardy *et al.*, 1997; Sclafani *et al.*, 2002; Hoang *et al.*, 2007). Studies to date have defined one kinetochore substrate for Cdc7, namely Ctf19 (Hinshaw *et al.*, 2017), a component of the COMA (Ctf19, Okp1, Mcm21, and Ame1) complex (Ortiz *et al.*, 1999). Cdc7-mediated phosphorylation of Ctf19 is required for its association with cohesin loaders Scc2/4 and the loading of cohesin to the *CEN* chromatin (Hinshaw *et al.*, 2017). Interestingly, Ctf19 interacts with Cse4, and this interaction is important for the recruitment of the COMA complex to *CEN* chromatin and maintenance of the functional integrity of the kinetochore (Ortiz *et al.*, 1999). A potential role for Cdc7-mediated phosphorylation of Cse4 in kinetochore function and chromosome segregation has not been characterized.

We here show that Cdc7 phosphorylates Cse4 in vitro and interacts in vivo with Cse4 in cell cycle-regulated manner. Cdc7 regulates the maintenance of Cse4 at the kinetochores as evident from the significant reduction of *CEN*-associated Cse4 in mitotic cells, a faster exchange of Cse4 at the metaphase kinetochores and defects in chromosome segregation in a *cdc7-7* strain. Cdc7-mediated Cse4 phosphorylation regulates faithful chromosome segregation as increased frequency of chromosome loss was observed in the nonphosphorylatable *cse4* mutant (*cse4-4A*). Moreover, constitutive association of kinase-dead variant of Cdc7 (*cdc7-kd*) with Cse4 at the kinetochore causes growth defects suggesting that Cdc7-mediated Cse4 phosphorylation is important for cell viability. In summary, we have identified Cse4 as a substrate for Cdc7, and shown that Cdc7-mediated phosphorylation of Cse4 contributes to high-fidelity chromosome segregation.

RESULTS

Cdc7 phosphorylates Cse4 in vitro

DDK enrichment has been observed at the budding yeast kinetochores (Natsume *et al.*, 2013; Hinshaw *et al.*, 2017) and proposed to regulate loading of *CEN* cohesion through phosphorylation of Ctf19 (Hinshaw *et al.*, 2017). Moreover, Ctf19 as well as other members of the COMA complex interact with Cse4, which is required for the *CEN* recruitment of COMA complex and kinetochore assembly (Ortiz *et al.*, 1999). Therefore, we examined whether Cdc7 kinase interacts with and phosphorylates Cse4 in vitro. We performed in vitro kinase assays with radiolabeled ATP using DDK (Cdc7/Dbf4 complex) and Cse4 purified from *Escherichia coli*. Cse4 was radiolabeled in the presence of DDK (Figure 1A). Moreover, Cse4 phosphorylation by DDK increased over time (Figure 1A). Control reaction performed without DDK complex did not show a signal (Figure 1A). Based on these results, we conclude that Cdc7 interacts with and phosphorylates Cse4 in vitro.

Cdc7 interacts with Cse4 in vivo in a cell cycle-dependent manner

The in vitro phosphorylation of Cse4 by Cdc7 prompted us to examine whether Cdc7 and Cse4 interact in vivo. We constructed a strain that expresses Flag-tagged Cdc7 and HA-tagged Cse4 from their endogenous promoters. Immunoprecipitation (IP) experiments were performed using protein extracts from logarithmically growing cultures. *F*luorescence *A*ctivated *C*ell *S*orting (FACS), examination of nuclear position, and cell morphology confirmed that the strain was in the logarithmic phase of growth (Figure 1B and Supplemental Figure S1). Western blot results showed an in vivo interaction of Cdc7 with Cse4 (Figure 1C). IP performed with Cdc7-Flag showed HA-Cse4 signal; reciprocal pull down with HA-Cse4 showed Cdc7-Flag signal (Figure 1C).

To determine whether the in vivo interaction of Cdc7 with Cse4 is cell cycle regulated, IP experiments were performed using cells in G1, S, and G2/M phase of the cell cycle. The cell cycle phase was confirmed by FACS, nuclear position, and cell morphology analyses (Figure 2A; Supplemental Figures S2, A and C, and Supplemental Figure S3). In agreement with previous studies (Jackson *et al.*, 1993), we observed an expression of Cdc7 in G1, S, and G2/M phases of the cell cycle (Figure 2B; Supplemental Figure S2, B and D). IP results showed an interaction between Cdc7 and Cse4 in the S-phase and G2/M, whereas no interaction of Cdc7 with Cse4 was detected in G1 despite the expression of Cdc7 and Cse4 in these cells (Figure 2B; Supplemental Figure S2, B and D). Next, we quantified the fraction of Cse4 pulled down in the IP of Cdc7. The maximum interaction of Cdc7 with Cse4 was observed in S-phase cells, which was ~2-fold higher than G2/M cells (Figure 2C). We conclude that in vivo interaction of Cdc7 with Cse4 is primarily observed in the S-phase and to some extent, in G2/M cells.

The cell cycle-dependent interaction of Cdc7 and Cse4 prompted us to examine whether association of Cdc7 with *CEN* chromatin is affected by the cell cycle. Hence, we performed chromatin immunoprecipitation (ChIP) experiments to determine the levels of Cdc7 at *CEN* chromatin in G1, S, and G2/M stages of the cell cycle (Figure 2D). The *CEN* enrichment of Cdc7 was observed in all three stages of the cell cycle; however, the enrichment levels were slightly lower in G2/M cells than those observed in G1 and S-phase cells (Figure 2D). No significant enrichment of Cdc7 was detected at a negative control (CON) region (Figure 2D). Taken together, our results show that the in vivo association of Cdc7 with Cse4 is cell cycle dependent; however, Cdc7 associates with *CEN* chromatin in all phases of the cell cycle.

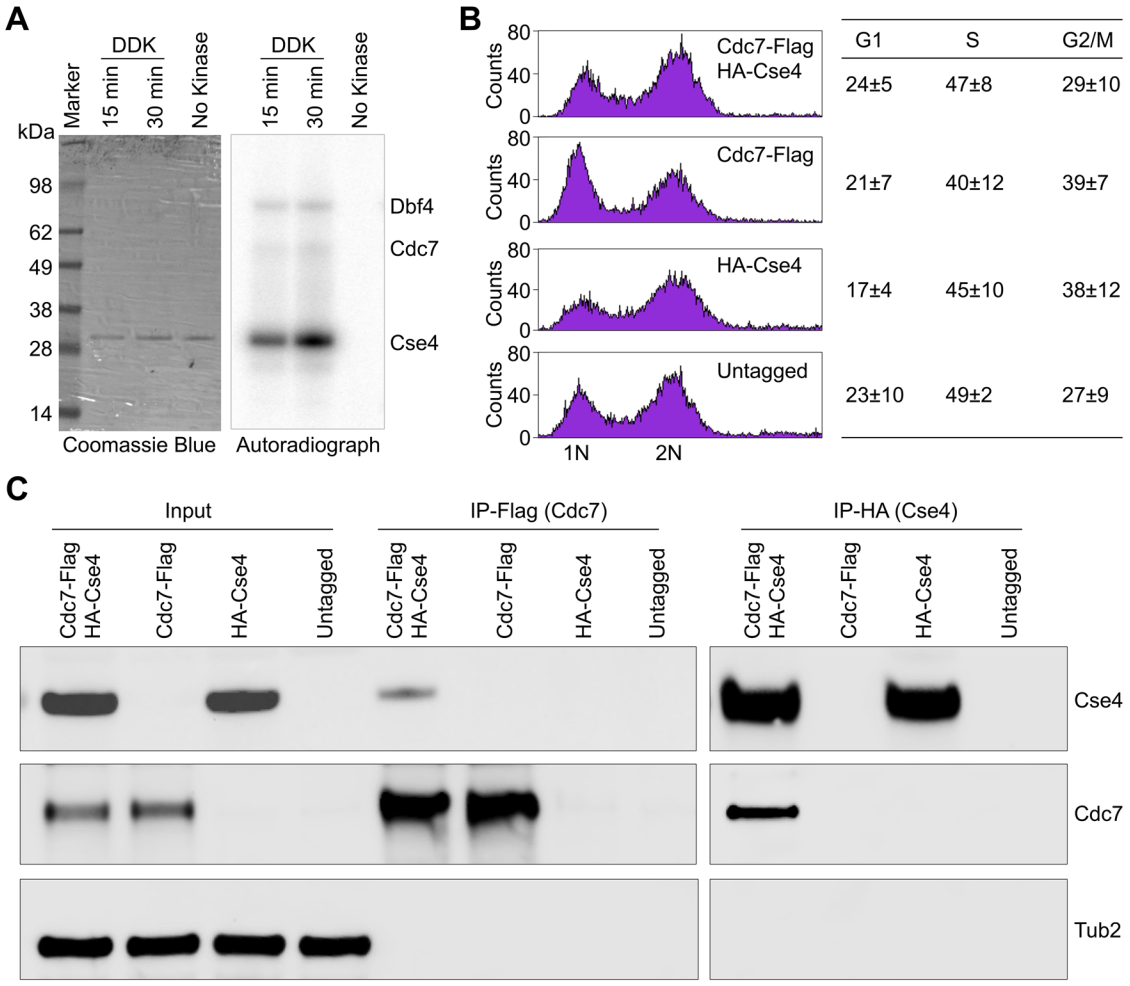

FIGURE 1: Cdc7 phosphorylates Cse4 in vitro and interacts with Cse4 in vivo. (A) In vitro kinase assay showing phosphorylation of Cse4 by Cdc7. (B) FACS profiles and morphological analyses of logarithmically growing strains. Average ± SD from three biological replicates are shown. Control (Untagged, RSY299), HA-Cse4 (YMB9337), Cdc7-Flag (YMB9509), and HA-Cse4 Cdc7-Flag (YMB9539) strains were grown in YPD at 25°C to logarithmic phase and whole cell extracts were prepared and used in IP experiments using α-Flag agarose and α-HA agarose. (C) Cdc7 interacts with Cse4 in vivo. Western blots from IP experiments showing in vivo interaction between Cdc7 and Cse4 in logarithmically growing cells. Control untagged strain did not show Cse4-Cdc7 interaction.

Cdc7 is required for stable maintenance of Cse4 at the kinetochore during mitosis

Cse4 recruitment to the *CEN* chromatin occurs in early S-phase coincident with the replication of *CEN* DNA (Newlon, 1988; Pearson *et al.*, 2004). Once recruited to kinetochores in early S-phase, Cse4 remains stably associated with it throughout the cell cycle (Pearson *et al.*, 2004; Wisniewski *et al.*, 2014). Moreover, Cdc7 kinase is essential for DNA replication initiation during S-phase of the cell cycle through *MCM2-7* helicase phosphorylation (Rossbach *et al.*, 2017). Given our findings that Cdc7 phosphorylates Cse4 in vitro and interacts with Cse4 in vivo during S-phase and G2/M stages of the cell cycle (Figures 1 and 2), we posited that Cdc7 may have a role either in recruitment and/or in maintenance of Cse4 at the *CEN* chromatin. Hence, we performed ChIP experiments to determine the *CEN* enrichment of Cse4 in the S-phase. Strains were grown to early logarithmic phase at 25°C, HU was added (to synchronize cells in the S-phase), and cultures were incubated at 25° and 37°C for 2 h. The well-characterized temperature-sensitive *cdc7-7* mutant does not have defects in the cell cycle at 23°C, shows low frequency of induced mutagenesis, and exhibits defects in DNA replication only at the nonpermissive temperature of 37°C (Hollingsworth *et al.*, 1992). Cell cycle synchronization in the S-phase was confirmed by FACS, nuclear position, and cell morphology analyses (Supplemental Figure S4, A–C). Western blot analysis showed that the protein levels of Cse4 in the S-phase were lower in *cdc7-7* than the wild-type strain at both the permissive (25°C) and after a shift to the nonpermissive temperature of 37°C (Figure 3A). The reduced protein levels of Cse4 in *cdc7-7* were not due to transcriptional defects as similar levels of *CSE4* RNA were detected in wild-type and *cdc7-7* strains (Supplemental Figure S4D). The reduced levels of endogenous Cse4 in the *cdc7-7* strain are consistent with our previous studies (Eisenstatt *et al.*, 2020). ChIP- quantitative PCR (qPCR) showed that the enrichment of Cse4 at *CEN* chromatin (*CEN1* and *CEN3*) is not significantly different between wild-type and *cdc7-7* strains at 25°C or 37°C (p value = >0.05; Figure 3B). There was no significant enrichment of Cse4 at the non-*CEN* negative control *ACT1* region (Figure 3B). These results show that despite the reduced protein levels of Cse4, its recruitment to the *CEN* chromatin during S-phase is not affected in *cdc7-7* strain.

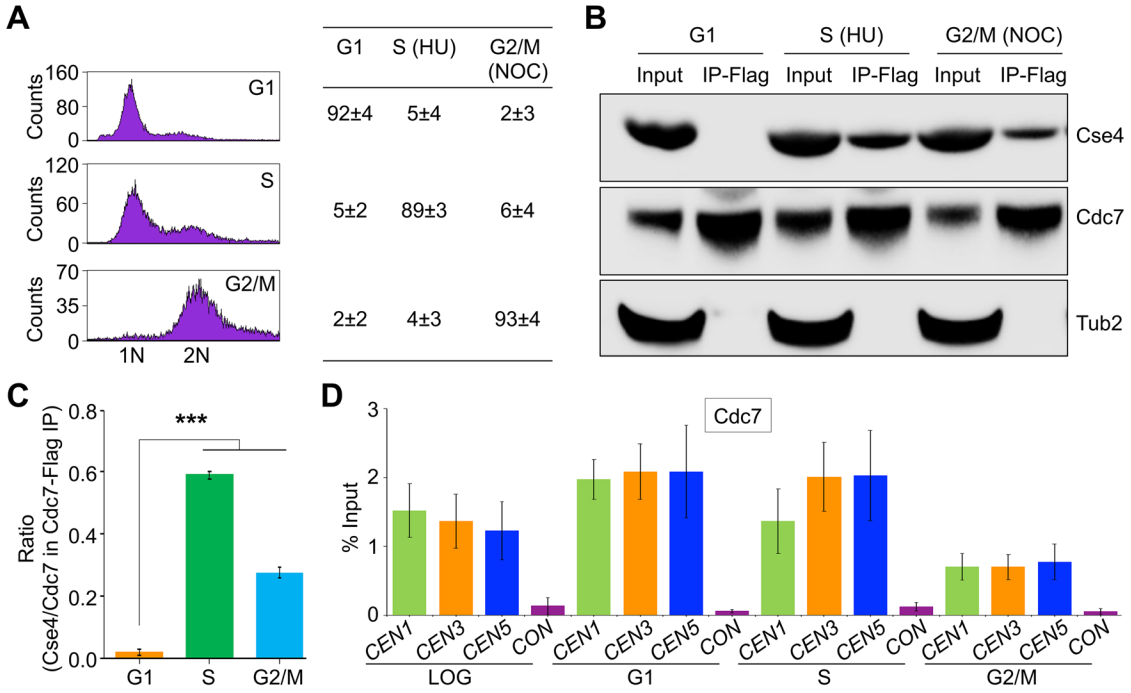

FIGURE 2: In vivo interaction of Cdc7 with Cse4 is regulated by the cell cycle independent of *CEN*-association of Cdc7. Strains carrying HA-Cse4 Cdc7-Flag (YMB9539) was grown in YPD at 25°C to early logarithmic phase and synchronized in G1, S, and G2/M stages of the cell cycle. Whole cell extracts were prepared and used in IP experiments using α-Flag agarose. (A) FACS profiles and morphological analyses showing synchronization in G1, S-phase, and G2/M stages of the cell cycle. Average ± SD from three biological replicates are shown. (B) Cdc7 interacts with Cse4 in the S-phase and G2/M cells but not in G1. Western blots from IP experiments showing in vivo interaction between Cdc7 and Cse4 in different stages of the cell cycle. (C) Enrichment levels of Cdc7 and Cse4 interaction in different stages of the cell cycle. Ratio of Cse4 to Cdc7 pulled down by IP experiments using Cdc7-Flag in G1, S, and G2/M cells. Enrichment levels were determined by quantification of Western blots using Image J (Schneider *et al.*, 2012). Average from three biological replicates ± SE are shown. ***p value < 0.0001, Student's t test. (D) Cdc7 associates with *CEN* chromatin throughout the cell cycle. ChIP for endogenously expressed Flag-tagged Cdc7 was performed from LOG, G1, S, and G2/M cultures of HA-Cse4 Cdc7-Flag strain (YMB9539) grown as described above with α-Flag agarose. Enrichment of Cdc7 at *CEN1*, *CEN3*, *CEN5*, and a negative control (*CON*) was determined by qPCR and is shown as % input. Average from three biological replicates ± SE. No statistically significant difference was observed between cell cycle stages based on the analysis of variance (p value > 0.05).

We next examined whether Cdc7 has a role in the maintenance of Cse4 at *CEN* chromatin during mitosis. ChIP experiments were done with wild-type and *cdc7-7* cells synchronized in G2/M. Strains were grown to early logarithmic phase at 25°C, nocodazole was added (to synchronize cells in G2/M), and cultures were incubated at 25° and 37°C for 2 h. Cell cycle synchronization in G2/M was confirmed by FACS, nuclear position, and cell morphology analyses (Supplemental Figure S5, A–C). Western blotting showed that the protein levels of Cse4 in G2/M were lower in *cdc7-7* than wild-type strain at permissive (25°C) and nonpermissive (37°C) temperatures (Figure 3C). The reduced protein levels of Cse4 in *cdc7-7* were not contributed by transcriptional defects as similar levels of *CSE4* RNA were detected in wild-type and *cdc7-7* strains (Supplemental Figure S5D). ChIP-qPCR showed that the enrichment of Cse4 at *CEN* chromatin (*CEN1* and *CEN3*) is not significantly different between wild-type and *cdc7-7* strains at 25°C (p value = >0.05; Figure 3D). However, enrichment of Cse4 at the *CEN* was reduced significantly in *cdc7-7* (~2.7–2.8% of input) compared with the levels observed in a wild-type strain (~3.2–3.3% of input) at 37°C (Figure 3D). No significant enrichment of Cse4 was detected at the non-*CEN ACT1* locus used as a negative control (Figure 3D). These results show that the maintenance of Cse4 at the *CEN* chromatin is affected in *cdc7-7* strains.

In an independent approach, we used cell biology to further examine the role of Cdc7 in maintenance of Cse4 at the *CEN* chromatin. We quantified the intensity of green fluorescent protein (GFP)-Cse4 foci at bioriented kinetochores in metaphase cells of wild-type and *cdc7-7* strains grown at 37°C for 2 h. Our results showed that the intensity of GFP-Cse4 foci at the kinetochores was reduced significantly in *cdc7-7* when compared with the wild-type strain (Figure 4, A and B). These results are consistent with the reduction of *CEN*-associated Cse4 in mitotic cells of *cdc7-7* strain (Figure 3D). Moreover, the difference in GFP-Cse4 intensity between wild type and *cdc7-7* was slightly higher than those detected by ChIP experiments (Figure 3D), which can be attributed to the two independent experimental approaches; for example, ChIP measured the levels of Cse4 at individual *CEN*s, whereas GFP-Cse4 signals were derived from the clustering of all 16 *CEN*s. Based on these results, we hypothesized that Cdc7 may regulate the stable association of Cse4 at the kinetochore. Hence, we examined the exchange of GFP-Cse4 at metaphase kinetochores using a fluorescence recovery after photobleaching (FRAP) assay (Pearson *et al.*, 2004). Wild-type and *cdc7-7* strains were grown at 37°C for 2 h and FRAP (pre and post) of GFP–Cse4-labeled centromeres was followed at 2-min intervals for 10 min. The average fluorescence recovery of GFP-Cse4 after photobleaching in the wild-type strain was low (~0.44% after 10 min),

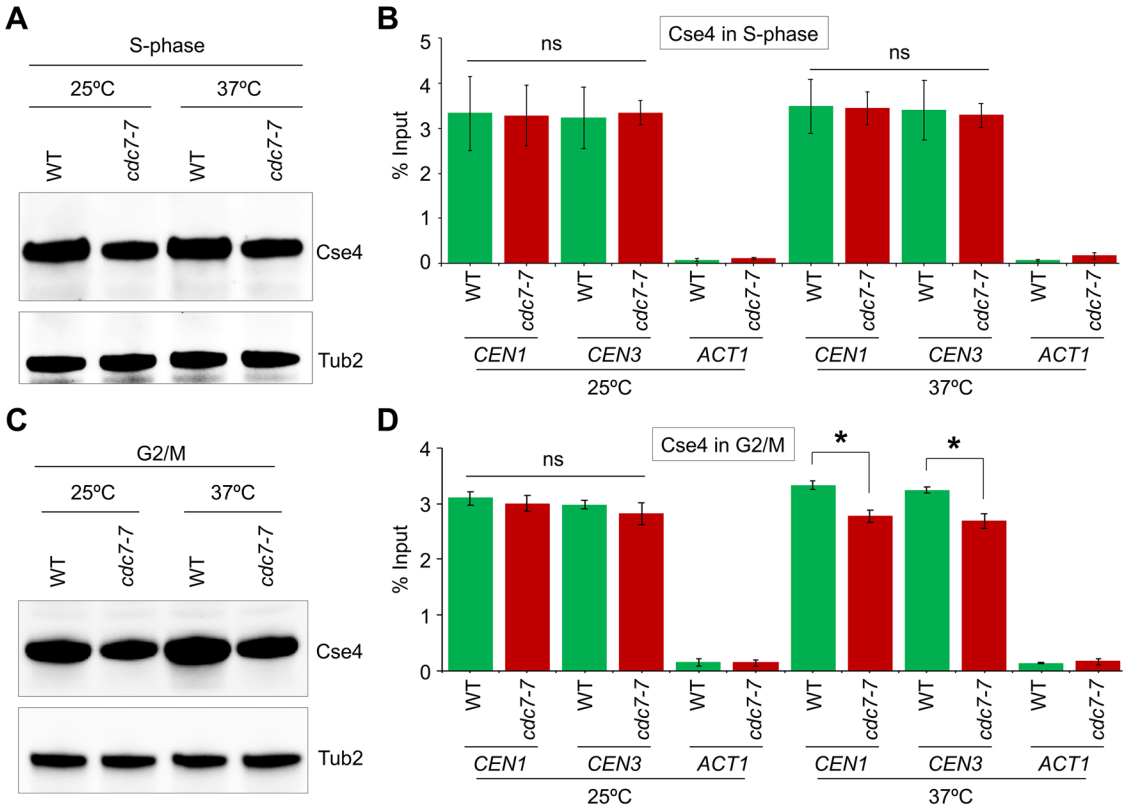

FIGURE 3: *CEN* recruitment of Cse4 in the S-phase is not affected but its maintenance at the *CEN* in G2/M is affected in a *cdc7-7* strain. (A) Protein expression of Cse4 is reduced in the S-phase of *cdc7-7* strain. Western blots showing protein levels of Cse4 in WT (YMB9337) and *cdc7-7* (YMB9338) strains synchronized in the S-phase with 0.2 M HU at permissive (25°C) and after 2 h shift to nonpermissive temperature (37°C). Tub2 used a loading control. (B) Cse4 localization and its levels at *CEN* chromatin in the S-phase are not affected in a *cdc7-7* strain. ChIP for endogenously expressed HA-tagged Cse4 from strains in A was performed using α-HA agarose. Enrichment of Cse4 at *CEN1*, *CEN3*, and a negative control (*ACT1*) was determined by qPCR and is shown as % input. Average from three biological replicates ± SE; ns = statistically not significant (p value > 0.05, Student's t test). (C) Protein expression of Cse4 is reduced in G2/M of *cdc7-7* strain. Western blots showing protein levels of Cse4 in WT (YMB9337) and *cdc7-7* (YMB9338) strains synchronized in G2/M with 20 µg/ml nocodazole at permissive (25°C) and after 2 h shift to nonpermissive temperature (37°C). Tub2 used a loading control. (D) The *CEN* maintenance of Cse4 in G2/M is affected in a *cdc7-7* strain. ChIP for endogenously expressed HA-tagged Cse4 from strains in C was performed using α-HA agarose. Enrichment of Cse4 at *CEN1*, *CEN3*, and a negative control (*ACT1*) was determined by qPCR and is shown as % input. Average from three biological replicates ± SE. *p value < 0.05; ns = statistically not significant, Student's t test.

implying that Cse4 is stably maintained at the kinetochore (Figure 4, A and C). These results are consistent with previous observations showing low levels of fluorescence recovery of GFP-Cse4 after photobleaching in metaphase cells (Pearson *et al.*, 2004; Lawrimore *et al.*, 2011). The average GFP-Cse4 fluorescence recovery in the *cdc7-7* strain was ~30-fold higher (~15% after 10 min), which was significantly faster than that observed in the wild-type strain (p value = < 0.05; Figure 4C). These results are consistent with the reduced levels of Cse4 at *CEN* chromatin (Figure 3D) and reduced intensity of GFP-Cse4 (Figure 4, A and B) in mitotic cells of the *cdc7-7* strain. We conclude that Cdc7 is required for stable maintenance of Cse4 at the kinetochore during mitosis.

cdc7-7 strains exhibit CIN phenotype

The rapid exchange and reduced levels of *CEN*-associated Cse4 in *cdc7-7* strains led us to examine the fidelity of chromosome segregation in this strain. CIN phenotype was determined by quantification of cells that retain a *CEN* plasmid (pRS415 *LEU2*) after growth in nonselective medium at the permissive temperature of 23°C. The retention of *CEN* plasmid in *cdc7-7* strain was about 7-fold lower than the wild-type strain (Figure 5), which is similar to that reported previously for kinetochore mutants (Kastenmayer *et al.*, 2005; Ma *et al.*, 2012). These results support a role for Cdc7 in preventing CIN.

Cdc7 kinase along with Dbf4 are essential for the initiation of DNA replication facilitated by phosphorylation of Cdc45 and Mcm2-7 complex (Lei *et al.*, 1997; Owens *et al.*, 1997; Weinreich and Stillman, 1999; Zou and Stillman, 2000; Bruck and Kaplan, 2009). Previous studies have shown that mutation in *MCM5* (*mcm5-bob1*) bypasses the requirement of Cdc7 for replication initiation and leads to suppression of temperature sensitivity and DNA replication defects in a *cdc7*-7 strain (Hardy *et al.*, 1997; Sclafani *et al.*, 2002; Hoang *et al.*, 2007). Hence, we examined if defects in DNA replication initiation contribute to the CIN phenotype in *cdc7-7* strain. We compared the frequency of *CEN* plasmid retention in wild-type, *cdc7-7*, *mcm5-bob1*, and *cdc7-7 mcm5-bob1* strains. Our results showed that *CEN* plasmid retention is similar between *mcm5-bob1* and wild-type strains (p value = 0.19). The *cdc7-7*

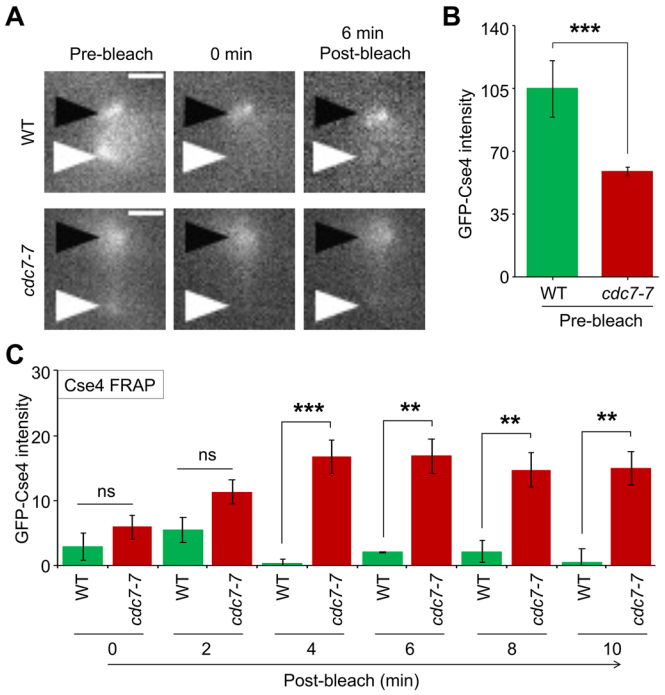

FIGURE 4: Cdc7 is required for the maintenance of Cse4 at metaphase kinetochores and faithful chromosome segregation. (A) Representative images showing the GFP-Cse4 intensity at metaphase kinetochores. Black arrows represent prebleached GFP-Cse4 foci and white arrows represent bleached GFP-Cse4 foci. The scale bar is 1 μm in length. (B) GFP-Cse4 intensity at kinetochores is reduced in metaphase cells of *cdc7-7* strain. WT (YMB11463) and *cdc7-7* (YMB11464) strains were grown and shifted for 2 h to nonpermissive temperature (37°C). Metaphase cells were selected based on spindle length measurements. GFP-Cse4 intensity was measured (prebleached) by microscopic observations of the cells after subtracting the intracellular background. ***p value < 0.0001, Student's t test. (C) Cse4 exchange at kinetochores is faster in metaphase cells of *cdc7-7* strains. Average GFP-Cse4 fluorescence recovery in metaphase cells of WT (YMB11463) and *cdc7-7* (YMB11464) grown as described in A at 0, 2, 4, 6, and 10 min postbleaching ± SE is shown. **p value < 0.01, ***p value < 0.001, ns = statistically not significant, Student's t test.

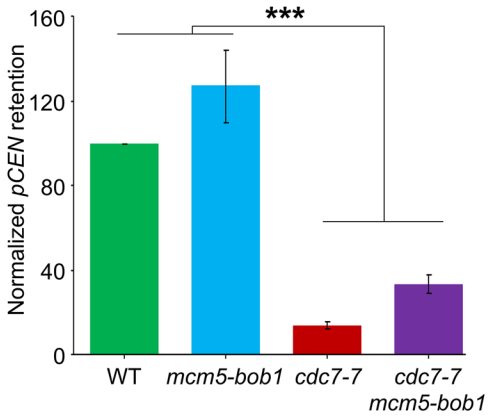

FIGURE 5: Increased *CEN* plasmid loss in *cdc7-7* strain. WT (YMB11623), *cdc7-7* (YMB11621), *mcm5-bob1* (YMB11624), and *cdc7-7 mcm5-bob1* (YMB11622) strains transformed with *CEN* plasmid (pRS415) were grown in medium selective (SC-Leu) for the plasmid (denoted as G_0) and then allowed to grow nonselectively in YPD for 10 generations (G_{10}). Equal number of cells from G_0 and G_{10} were plated on YPD and SC-Leu plates at 23°C. Plasmid retention was measured by the ratio of colonies grown on SC-Leu/YPD. The ratio from G_{10} was divided by the ratio from G_0 and normalized to a value of 100 for the WT strain. Average from three biological experiments ± SE is shown. ***p value < 0.001, Student's t test.

mcm5-bob1 shows higher *CEN* plasmid retention compared with the *cdc7-7* strain; however, the frequency of *CEN* plasmid retention in *cdc7-7 mcm5-bob1* is significantly lower than the wild-type or *mcm5-bob1* strains (p value = < 0.01; Figure 5). Based on these results, we conclude that the CIN phenotype of *cdc7-7* strains is not solely due to defects in replication initiation.

Constitutive association of a kinase-dead variant of Cdc7 (*cdc7-kd*) with Cse4 at the kinetochores causes growth defects and lethality

We used the synthetic physical interaction (SPI) approach (Olafsson and Thorpe, 2015) to gain further insight into the activity of Cdc7 at the kinetochore and determine the physiological significance of Cdc7 and Cse4 interaction. The SPI system can uncover regulatory phenotype by forcibly and constitutively associating a regulator with potential targets (Olafsson and Thorpe, 2015). SPI is based on the growth inhibition due to forced association of two proteins, one of which is GFP-tagged, and the second protein fused to a GFP-binding protein (GBP). This approach has led to the identification of novel regulators for kinetochore and spindle pole body (centrosome) function (Olafsson and Thorpe, 2015; Berry *et al.*, 2016; Howell *et al.*, 2019) and an interaction of DDK with kinetochore protein Mtw1 (Olafsson and Thorpe, 2015; Klemm *et al.*, 2020; Olafsson and Thorpe, 2020). We used SPI to examine the outcome of forced interaction of Cdc7 and a kinase-dead version of Cdc7 (cdc7-kd) fused to GBP (Rothbauer *et al.*, 2006; Fridy *et al.*, 2014) and a red fluorescent protein (RFP) with GFP-tagged Cse4 (Figure 6A). Plasmids pCdc7 and pGBP were used as controls for expression of either Cdc7 or GBP alone. It is noted that all strains contain endogenous Cdc7, which was not tagged. Growth of the strains with fusion of Cdc7 or Cdc7-kd with the GFP-Cse4 was assessed using colony size as a surrogate for growth, as previously described (Olafsson and Thorpe, 2017). We found that cdc7-kd-GBP but not Cdc7-GBP exhibits SPI when forced to associate with GFP-Cse4 (Figure 6, B and C). We next examined the consequence of forced association of cdc7-kd-GBP with GFP-Cse4 at the kinetochore using fluorescence imaging (Supplemental Figure S6A). We observed that intensity of GFP-Cse4 foci was reduced on forced association of the kinase-dead version (cdc7-kd-GBP) with GFP-Cse4 (Supplemental Figure S6B). We next examined if the reduced intensity of GFP-Cse4 correlated with the cell cycle stage by examining unbudded and budded cells based on nuclear position and cell morphology. Our results showed that decreased intensity of GFP-Cse4 foci in cdc7-kd-GBP strain was not cell cycle dependent as similar reduction in GFP-foci intensity was observed in unbudded and budded cells (Supplemental Figure S6C). These results are consistent with reduced levels of GFP-Cse4 observed at metaphase kinetochores in a *cdc7-7* strain (Figure 4, A and B) and show that perturbed Cdc7-mediated phosphorylation of Cse4 contributes to growth defects and reduced intensity of GFP-Cse4 foci (Supplemental Figure S6).

We next examined the growth phenotype of forced association of Cdc7-GBP or cdc7-kd-GBP with 89 different GFP-tagged kinetochore-related proteins. Selective ploidy ablation (SPA; Reid *et al.*, 2011) was used to transform pCdc7-GBP or pCdc7-kd-GBP into 89 GFP-tagged kinetochore proteins including Cse4 (with pCdc7 and pGBP as controls). Again, this screen identified a growth defect of

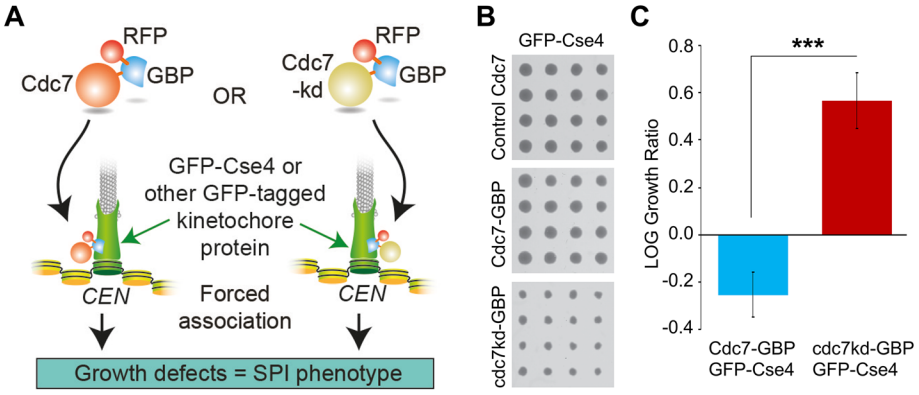

D

Bait	Query protein (GFP tagged)
Cdc7-GBP-RFP	Ame1, Dad4, Ipl1, Sli15, Spc24, and Spc42
Cdc7kd-GBP-RFP	Ame1, Bub1, Cdc20, **Cse4**, Cnn1, Ctf19, Htb1, Kre28, Sli15, and Spc25

FIGURE 6: Constitutive association of a kinase-dead variant of Cdc7 (cdc7-kd) with Cse4 at the kinetochores causes growth defects. (A) Schematic of SPI assay. (B) Representative images of the scanned plates from the SPI screen with GFP-Cse4 show 16 replicates for each strain (rows) and plasmid (columns) combination. (C) The colony sizes in B were measured and LGRs plotted for the strains carrying GFP-Cse4 and Cdc7-GBP or cdc7-kd-GBP. Error bars indicate SD from the mean. ***p value < 0.0001, Student's t test. (D) List of proteins showing SPI phenotype when associated constitutively with Cdc7-GBP and cdc7-kd-GBP.

GFP-Cse4 with pCdc7-kd-GBP (Supplemental Table S1). The SPI screen also identified several other GFP-tagged proteins that exhibited a growth defect when associated with either Cdc7-GBP and/or cdc7-kd-GBP (Supplemental Table S1). Cdc7-GBP produced a growth defect with six GFP proteins (Ame1, Dad4, Ipl1, Sli15, Spc24, and Spc42), whereas the screen with cdc7-kd-GBP identified 10 SPI partners (Ame1, Bub1, Cdc20, Cse4, Cnn1, Ctf19, Htb1, Kre28, Sli15, and Spc25) (Figure 6D). Two proteins (Ame1 and Sli15) exhibited SPI phenotypes in both of these screens (Figure 6D). SPI interactions of Cdc7 with other kinetochore proteins provide an opportunity for future research. Taken together, these results show that constitutive association of cdc7-kd-GBP with GFP-Cse4 at the kinetochores is detrimental to growth with reduced intensity of GFP-Cse4 foci.

Cse4 phosphorylation deficient mutants exhibit defects in chromosome segregation

Previous studies have shown that the consensus target amino acid sequences for DDK is serine (S) or threonine (T) followed by a negatively charged amino acid residue, aspartic acid (D) or glutamic acid (E) (Cho *et al.*, 2006; Montagnoli *et al.*, 2006; Charych *et al.*, 2008; Randell *et al.*, 2010; Hiraga *et al.*, 2014). In addition, DDK also carries out priming-dependent phosphorylation of S or T when these amino acid residues are followed by a phosphorylated S or T (Sasanuma *et al.*, 2008; Wan *et al.*, 2008; Randell *et al.*, 2010). Our sequence analysis identified seven potential DDK target amino acid residues within Cse4 in which four were consensus target sequences (S148, T149, T166, and S190) and three were priming-dependent residues (S9, S10, and S14) previously shown to be phosphorylated by pololike kinase Cdc5 (Mishra and Basrai, 2019; Mishra *et al.*, 2019). The four direct target residues occur in the histone-fold domain, whereas three priming-dependent residues are located within the N-terminus of Cse4. All of these seven residues of Cse4 are evolutionarily conserved among different fungi with point centromeres (Figure 7A). To define the significance of these potential DDK target sequences, we constructed *CSE4* alleles in which we mutated either all the seven or four putative DDK target amino acid residues to alanine (*cse4-7A* and *cse4-4A*, respectively) and examined the consequence on loss of a reporter chromosome fragment (CF). The cse4-4A and cse4-7A proteins were expressed at levels similar to the wild-type Cse4 (Figure 7B). The loss of CF was measured using the colony color assay (Spencer *et al.*, 1990). Our results showed significantly higher frequency of CF loss in *cse4-4A* and *cse4-7A* than the wild-type strain; loss of CF was similar between *cse4-4A* and *cse4-7A* strains (Figure 7C). These results support a role for Cdc7-mediated phosphorylation of Cse4 in faithful chromosome segregation.

To determine the effects of constitutive phosphorylation of Cse4 by Cdc7, we constructed the phospho-mimetic *cse4* mutant, in which all four DDK target phosphorylated residues were changed to aspartic acid (*cse4-4D*). We examined the ability of *cse4-4D* to complement the growth of a *cse4Δ* strain after loss of *CSE4/URA3* plasmid by counterselection on medium containing 5′-fluoro-orotic acid (5-FOA). Strains with Cse4 grew robustly on plates containing 5-FOA, whereas strains carrying *cse4-4D* did not exhibit growth on 5-FOA plates (Figure 7D). The lethality of *cse4-4D* precluded further analysis of this mutant.

DISCUSSION

Cdc7 kinase associates with *CEN* and modulates the timely replication of *CEN* DNA and loading of the cohesin components (Natsume *et al.*, 2013; Hinshaw *et al.*, 2017). Studies to date have identified Ctf19 as the only kinetochore substrate for Cdc7 (Hinshaw *et al.*, 2017). In this study, we uncovered that evolutionarily conserved *CEN*-specific histone H3 variant, Cse4 is a bonafide substrate of Cdc7. Our results showed that Cdc7 phosphorylates Cse4 in vitro and interacts with Cse4 in vivo in a cell cycle-regulated manner with maximum interaction in the S-phase and to some extent in G2/M but not in G1. Previous studies have shown reduced DDK activity in G1 cells (Oshiro *et al.*, 1999). Consistent with previous results (Natsume *et al.*, 2013; Hinshaw *et al.*, 2017), ChIP experiments showed that *CEN* association of Cdc7 is not cell cycle regulated. The Cdc7-dependent phosphorylation of Cse4 is physiologically important because constitutive association of a kinase-dead variant (*cdc7-kd*) with Cse4 results in growth defects. Errors in chromosome segregation and reduction in *CEN*-associated Cse4 were observed in a catalytically inactive *cdc7-7* strain. Moreover, a phosphomimetic mutant (*cse4-4D*) that did not rescue the growth of a *cse4Δ* strain implies that constitutive phosphorylation of Cse4 is also detrimental to cell growth. Taken together, these results suggest that the cell cycle-mediated, dynamic phosphorylation of Cse4 by Cdc7 is important for the maintenance of cell viability, proper kinetochore function, and faithful chromosome segregation.

Our studies have now uncovered at least three protein kinases (i.e., Cdc7, Cdc5, and Ipl1) that are involved in phosphorylation of Cse4 (Boeckmann *et al.*, 2013; Mishra and Basrai, 2019; Mishra *et al.*, 2019). Unlike Cse4 which interacts with Cdc7 primarily in the

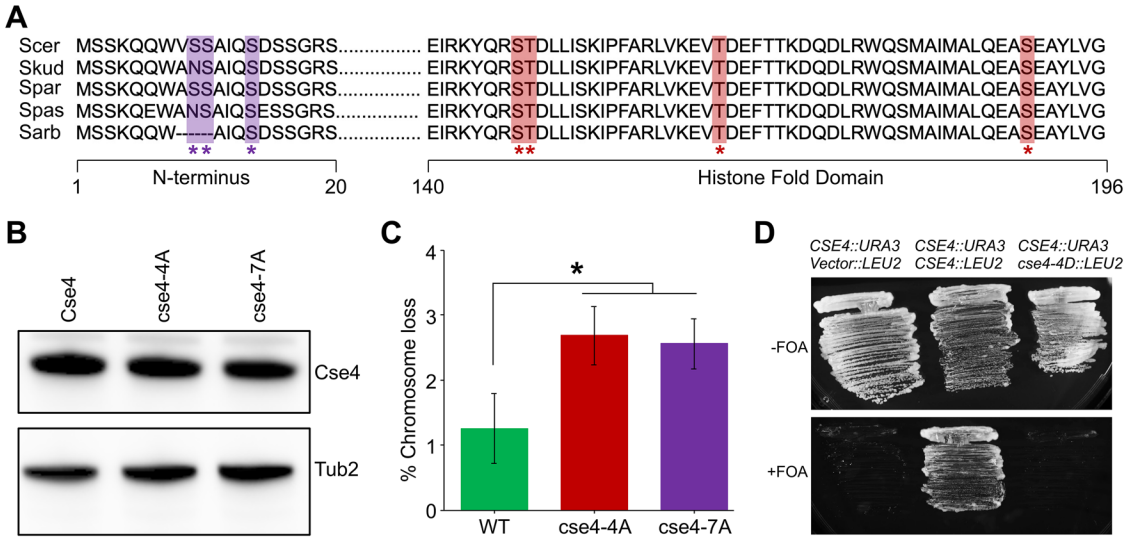

FIGURE 7: Cdc7-mediated phosphorylation of Cse4 contributes to faithful chromosome segregation. (A) In silico analysis identified Cse4 amino acids that are potential phosphorylation targets for Cdc7 (shown in shaded color with an asterisk). Clustal-W alignment showed that predictive Cdc7 target amino acid residues of Cse4 are evolutionarily conserved in yeasts with point *CEN* and related species. Scer, *Saccharomyces cerevisiae*; Skud, *Saccharomyces kudriavzevii*; Spar, *Saccharomyces paradoxus*; Spas, *S. pastorianus*; and Sarb, *Schefflera arboricola*. (B) Protein expression of Cse4 and its variant (*cse4-4A* and *cse4-7A*) as determined by Western blotting. Tub2 used as a loading control. (C) Errors in chromosome segregation are increased in phospho-deficient mutants of Cse4. Frequency of CF loss in wild-type (YMB11474), *cse4-4A* (YMB11475), and *cse4-7A* (YMB11476) strains was determined using a colony color assay as described in *Materials and Methods*. About 1200 colonies from three independent transformants were counted and average from three biological experiments ± SE is shown. **p* value < 0.05, Student's *t* test. (D) Phosphomimetic Cse4 mutant (*cse4-4D*) is unable to complement the growth defect of *cse4Δ* strain. Wild-type strain with *CSE4::URA3* (pRB199) was transformed with *vector::LEU2* (YMB11627), *CSE4::LEU2* (YMB11626), or *cse4-4D::LEU2* (YMB11625). Strains were plated on synthetic medium without or with counterselection for *URA3* by 5-FOA and incubated for ~3 d at 25°C.

S-phase, an interaction of Cse4 with Cdc5 is observed in G2/M cells (Mishra *et al.*, 2019). Cdc5-mediated phosphorylation of Cse4 maintains kinetochore integrity and chromosome transmission fidelity (Mishra and Basrai, 2019; Mishra *et al.*, 2019). Ipl1-mediated phosphorylation of Cse4 leads to destabilization of defective kinetochores to promote proper kinetochore biorientation (Boeckmann *et al.*, 2013; Mishra and Basrai, 2019). Our results of Cdc7-Cse4 interaction in the S-phase and its consequences on CIN and growth suggest a temporal regulation of Cse4 phosphorylation to maintain chromosomal stability. Although one protein kinase may be sufficient to phosphorylate its substrate, multiple protein kinases have increasingly been found to be involved in modulating a substrate in response to physiological changes during the cell cycle. For example, cyclin-dependent kinase (Cdk) and Cdc7 kinase function synergistically in phosphorylation of Mcm2 for regulation of DNA replication in human cells (Cho *et al.*, 2006). Similarly, Cdc28 and Cdc5 work together for the phosphorylation of Swe1 and the condensin complex in budding yeast (Asano *et al.*, 2005; St-Pierre *et al.*, 2009; Robellet *et al.*, 2015). Furthermore, Cdk, meiosis-specific kinase (Ime2), and Cdc5 phosphorylate several components of helicase-loaders and an essential helicase-activation protein Sld2 in order to block DNA replication between two meiotic cell divisions (Phizicky *et al.*, 2018). The involvement of multiple protein kinases in phosphorylation of Cse4 may allow for temporal and stringent control of kinetochore structure and function during the cell cycle. It is possible that these kinases may create a phosphorylation gradient at the kinetochores as proposed previously (Fuller *et al.*, 2008; Lampson and Cheeseman, 2011) in order to ensure the ordered assembly of kinetochore components, establish the correct kinetochore biorientation, and monitor the architectural fidelity of kinetochores during mitosis that are prerequisite for high-fidelity chromosome segregation. However, it is unclear how these protein kinases specifically recognize Cse4 and how they coordinate with the other components involved in Cse4 phosphorylation and dephosphorylation pathway(s), which need to be further investigated.

Our in silico analysis revealed seven putative sites for Cdc7 phosphorylation in Cse4. Four of these sites are consensus target residues (S148, T149, T166, and S190) located in the evolutionarily conserved C-terminus histone fold domain (HFD) of Cse4 (Meluh *et al.*, 1998; Keith *et al.*, 1999), whereas three sites are priming-dependent residues (S9, S10, and S14) clustered in the N-terminus of Cse4 (Ortiz *et al.*, 1999). Remarkably, Cse4 target sites phosphorylated by Cdc5 and Ipl1 are clustered within the N-terminus of Cse4 (Boeckmann *et al.*, 2013; Mishra and Basrai, 2019; Mishra *et al.*, 2019), while all four Cdc7 consensus target sites are located within the C-terminus HFD of Cse4, a domain that is essential for localization and maintenance of Cse4 at the *CEN* chromatin (Meluh *et al.*, 1998; Keith *et al.*, 1999). In agreement with the defined role of Cse4 HFD in kinetochore assembly (Meluh *et al.*, 1998; Keith *et al.*, 1999), we found that Cdc7-mediated phosphorylation of Cse4 is important for the maintenance of Cse4 levels at the kinetochores. Reduced levels of Cse4 at the *CEN* chromatin in G2/M cells and a faster exchange of Cse4 at the metaphase kinetochores were observed in a catalytically inactive *cdc7-7* strain or when a catalytically inactive version of Cdc7 was constitutively recruited to Cse4. Moreover, defects in Cdc7-mediated Cse4 phosphorylation causes increased errors in chromosome segregation (*cse4-4A* and *cse4-7A*), suggesting that Cse4 phosphorylation is important for the maintenance of

kinetochore integrity during mitosis. Interestingly, HFD of Cse4 interacts with histone H4 in the *CEN* nucleosome (Smith *et al.*, 1996; Glowczewski *et al.*, 2000) and the HFD mutants of Cse4 (*cse4-1* and *cse4-111*) exhibit a weakened interaction with histone H4 and defects in chromosome segregation (Stoler *et al.*, 1995; Smith *et al.*, 1996; Glowczewski *et al.*, 2000). Future studies should help us understand how the interaction of Cse4 with H4 affects the phosphorylation of Cse4 and modulates kinetochore assembly and faithful chromosome segregation.

In summary, we have shown that Cdc7 phosphorylates in vitro and interacts in vivo with Cse4 in a cell cycle-dependent manner for maintenance of Cse4 at mitotic kinetochores. We provide the first evidence for a functional role for Cdc7-mediated phosphorylation of Cse4 in cell viability and faithful chromosome segregation. It is notable that Cdc7/Dbf4 associates with the *CEN* (Wu *et al.*, 2016); however, it remains unexplored whether CENP-A is a direct substrate for Cdc7 in human cells. Results from our SPI screen provide an additional opportunity to investigate the physiological role for the interaction of Cdc7 with other kinetochore substrates, most of which are evolutionarily conserved. Identification and characterization of additional Cdc7 substrates at yeast and human kinetochores will allow us to better understand the role of phosphorylation of kinetochore proteins in the assembly of a functional kinetochore for faithful chromosome segregation and how errors in these pathways contribute to CIN observed in many cancers.

MATERIALS AND METHODS

Media, yeast strains, and plasmids

Yeast strains were grown in yeast peptone dextrose (YPD) medium (1% yeast extract, 2% Bacto-peptone, 2% glucose) or in supplemented minimal medium with 2% glucose, with amino acid dropout depending on the selection needed for the plasmids being used. For complementation assay, strains were plated on synthetic medium without or with counterselection for *URA3* by 5-FOA. A list of yeast strains, plasmids, and PCR primers used in this study are shown in Tables 1 and 2.

In vitro kinase assay

In vitro kinase assay was carried out using Cse4 produced in *E. coli* and purified by Sephacryl-S200 chromatography as described previously (Luger *et al.*, 1997; Boeckmann *et al.*, 2013). Cse4 was phosphorylated in vitro using purified DDK (Cdc7 and Dbf4) (Weinreich and Stillman, 1999) in 20-µl reaction volume containing 1 µg Cse4, 20 ng DDK, 25 mM Tris-HCl, pH 7.5, 2 mM dithiothreitol, 10 mM MgCl2, 0.5 mM EDTA, 100 µM ATP, and 1 µCi of [γ-^{32}P]ATP. Reactions were incubated at 30°C for 15 and 30 min, stopped with 5 µl of 4× NuPAGE LDS loading buffer (Life Technologies, Grand Island, NY), and heated at 95°C for 5 min. Assay containing all the reagents except the DDK (no kinase) was used as control. The samples were separated on 4–12% Bis-Tris SDS-polyacrylamide gels (Invitrogen), stained with Coomassie blue, and radiolabeled proteins were detected using a Storm Detector Model 860 (Molecular Dynamics, USA).

Cell cycle synchronization, IP, and Western blotting

Strains were grown in YPD to early logarithmic phase at 25°C, treated for 2 h with 0.2 M hydroxyurea (HU, H8627, Sigma) to arrest cells in the S-phase, 20 µg/ml nocodazole (M1404, Sigma) to arrest cells in G2/M, and 75 min after release from G2/M arrest to capture cells in G1. FACS analysis was performed to confirm the cell cycle arrest using a BD FACSort flow cytometer and Cell Quest software (BD Biosciences, Boston, MA), and cell cycle stages were determined based on nuclear position and cell morphology examination of propidium iodide-stained cells using the Zeiss Axioskop 2 microscope (Carl Zeiss, USA) following the methodologies as described previously (Calvert and Lannigan, 2010). IP experiments were performed with whole cell extracts using methodologies as described previously (Mishra *et al.*, 2011; Mishra *et al.*, 2018). IP experiments were performed using α-Flag agarose (A2220, Sigma Aldrich), and α-HA agarose (A2095, Sigma Aldrich) and immunoprecipitates were eluted with Flag-peptides (F3290, Sigma Aldrich) and HA-peptides (I2149, Sigma Aldrich), respectively. Total Protein extracts were prepared with the trichloroacetic acid protein precipitation method (Kastenmayer *et al.*, 2005), and protein levels were quantified using Bio-Rad DC protein quantitation assay (Bio-Rad Laboratories, Hercules, CA). Protein samples were separated by SDS–PAGE on 4–12% Bis-Tris SDS-polyacrylamide gels and transferred to nitrocellulose membrane, and Western blotting was performed as described previously (Boeckmann *et al.*, 2013). Primary antibodies used for Western blotting were α-HA (H6908, Sigma Aldrich), α-Flag (F3165, Sigma Aldrich), α-HA (12CA5, Roche), and α-Tub2 (custommade by the Basrai laboratory). Secondary antibodies used were HRP–conjugated sheep α-rabbit IgG (NA934V) and HRP–conjugated sheep α-mouse IgG (NA931V) from Amersham Biosciences (UK).

ChIP and qPCR experiments

ChIP experiments were done in three biological replications using the protocol and reagents as described previously (Mishra *et al.*, 2007; Mishra *et al.*, 2011). Strains for Cdc7 ChIP were grown in YPD at 25°C and synchronized in G1, S, and G2/M stages of the cell cycle as described for the IP experiments. Strains for Cse4 ChIP were grown in YPD at 25°C to early logarithmic phase. In this culture, we added HU (0.2 M) to synchronize cells in the S-phase or nocodazole (20 µg/ml) to synchronize cells in G2/M stages of the cell cycle, and cultures were incubated at permissive (25°C) and nonpermissive (37°C) temperatures for 2 h. Protein–DNA complexes were captured using α-Flag agarose (A2220, Sigma Aldrich) and α-HA agarose (A2095, Sigma Aldrich), washed, and processed as described previously (Mishra *et al.*, 2007; Mishra *et al.*, 2011). ChIP-qPCR was performed using Fast SYBR Green Master Mix in a 7500 Fast Real Time PCR System (Applied Biosystems, Foster City, CA) with amplification conditions as follows: 95°C for 20 s, followed by 40 cycles of 95°C for 3 s and 60°C for 30 s. The enrichment shown as percent input was calculated from three biological replicates of ChIP-qPCR experiments using the $_{\Delta\Delta}C_T$ method (Livak and Schmittgen, 2001).

FRAP experiments

GFP-Cse4 FRAP experiments were performed using cells grown to logarithmic phase of growth at room temperature and shifted to 37°C for 2 h. Imaging of metaphase cells was done as described previously (Chen *et al.*, 2000; Maddox *et al.*, 2000). The positions of kinetochores (GFP-Cse4) and spindle pole bodies (Spc29-RFP) were used as live cell markers for the cell cycle stage to identify cells in metaphase. One cluster of GFP-Cse4 fluorescence was photobleached with a short 35-ms exposure of focused 488-nm laser light in metaphase cells. A seven-plane fluorescence Z series (0.3-µm steps) was obtained immediately after laser exposure to measure the fluorescence photobleaching and recovery as previously described (Pearson *et al.*, 2004). GFP-Cse4 fluorescence intensities were determined by collecting the mean intensity by finding the mean pixel value of a region that fully encompassed the localized fluorescence. The size of this region varied from 4 × 5 pixels to 13 × 13 pixels. The total GFP-Cse4 fluorescence intensity was determined by subtracting the intracellular background levels.

(A) *S. cerevisiae* strains		
Strain	**Genotype**	**Reference**
RSY299	*MATα his3 leu2 trp1 ura3*	R. Sclafani
YMB9337	*MATα his3 leu2 trp1 ura3 cse4Δ::6His-3HA-CSE4::mx4NAT*	This study
YMB9338	*MATα leu2 trp1 his3 ura3 cdc7-7 cse4Δ::6His-3HA-CSE4::mx4NAT*	This study
YMB9509	*MATa his3-Δ200 HIS::pCu-lac1-GFP leu2-3,112::lacO::LEU2 ura3-52:: OsTIR1-9myc::URA3 CDC7-FLAG-AID::HYG*	Basrai lab
YMB9539	*MATα his3 leu2 trp1 ura3 cse4Δ::6His-3HA-CSE4::mx4NAT CDC7-AID-6FLAF::Hyg*	Basrai lab
YMB11463	*MATa ura3-52 trp1Δ63 leu2Δ1 lys2-801 his3Δ200 473A Spc29RFP:Hb cse4Δ::6His-GFP-CSE4::mx4NAT CDC7:G418*	This study
YMB11464	*MATa ura3-52 trp1Δ63 leu2Δ1 lys2-801 his3Δ200 473A Spc29RFP:Hb cse4Δ::6His-GFP-CSE4::mx4NAT cdc7-7:G418*	This study
YMB11474	*MATα ura3-52 lys2-801 ade2-101 trp1Δ63 his3Δ200 leu2Δ1 CFIII (CEN3L.YPH278) HIS3 SUP11 3HA-CSE4::NAT*	This study
YMB11475	*MATα ura3-52 lys2-801 ade2-101 trp1Δ63 his3Δ200 leu2Δ1 CFIII (CEN3L.YPH278) HIS3 SUP11 3HA-cse4-4A::NAT*	Phil Hieter
YMB11476	*MATα ura3-52 lys2-801 ade2-101 trp1Δ63 his3Δ200 leu2Δ1 CFIII (CEN3L.YPH278) HIS3 SUP11 3HA-cse4-7A::NAT*	This study
YMB11621	*MATα leu2 trp1 his3 1 ura3 cdc7-7 CEN Vector::LEU2 (pRS415)*	This study
YMB11622	*MATα leu2 trp1 his3 1 ura3 cdc7-7 mcm5-P83L (mcm5–bob1-2) CEN Vector::LEU2* (pRS415)	This study
YMB11623	*MATα his3 leu2 trp1 ura3 CEN Vector::LEU2 (pRS415)*	This study
YMB11624	*MATα ura3 leu2 trp1 his3 bob1-2 (mcm5-P83L) CEN Vector::LEU2 (pRS415)*	This study
YMB11625	*MATα his3Δ1 leu2Δ0 met15Δ0 ura3Δ0 cse4Δ::Km pRS416-3HA-CSE4 (pRB199) pRS415-cse4-4D (pMB2001)*	This study
YMB11626	*MATα his3Δ1 leu2Δ0 met15Δ0 ura3Δ0 cse4Δ::Km pRS416-3HA-CSE4 (pRB199) pRS415-CSE4 (pMB1725)*	This study
YMB11627	*MATα his3Δ1 leu2Δ0 met15Δ0 ura3Δ0 cse4Δ::Km pRS416-3HA-CSE4 (pRB199) CEN Vector::LEU2 (pRS415)*	This study
W8164-2B	*MATα CEN1-16::GAL-Kl-URA3*	(Reid *et al.*, 2011)
GFP strains	*MATa his3Δ1 leu2Δ0 met15Δ0 ura3Δ0 ORF-GFP::HIS3MX6*	(Huh *et al.*, 2003)

(B) List of plasmids		
Plasmid	**Description**	**Reference**
pRS415	*CEN Vector::LEU2*	(Sikorski and Hieter, 1989)
pRB199	*CEN 3HA-CSE4::URA3*	R. Baker
pMB1725	*CEN CSE4::LEU2*	Basrai lab
pMB2001	*CEN cse4-4D::LEU2*	This study
pHT835	*pCUP1 Cdc7 LEU2*	This study
pHT836	*pCUP1 Cdc7-GBP LEU2*	This study
pHT837	*pCUP1 cdc7KD-GBP LEU2*	This study
pHT4	*pCUP1 GBP LEU2*	(Olafsson and Thorpe, 2015)

TABLE 1: List of strains and plasmids used in this investigation.

CEN plasmid retention and chromosome segregation assays

The plasmid retention assays were carried out following the procedures as described previously (Au *et al.*, 2020). Briefly, strains were transformed with a *CEN* plasmid (pRS415 *LEU2*) and transformants were grown selectively in 1× SC-Leu with 2% glucose at the permissive temperature of 23°C. Cells were plated on 1× SC-Leu with 2% glucose and YPD plates (0 generation, used as a control). Cells were then inoculated into YPD medium and allowed to grow nonselectively for 10 generations at 23°C. Cells after 10 generations of growth were plated on 1× SC-Leu with 2% glucose and YPD plates as above (10 generations). Plasmid retention represents the ratio of the number of colonies grown on SC-Leu over YPD after 10 generations of nonselective growth. The ratio from 10 generations was divided by the ratio from 0 generation (control) and normalized to a

Locus	Primer F (5′–3′)	Primer R (5′–3′)	Reference
CEN1	CTCGATTTGCATAAGTGTGCC	GTGCTTAAGAGTTCTGTACCAC	(Choy *et al.*, 2011)
CEN3	GATCAGCGCCAAACAATATGG	AACTTCCACCAGTAAACGTTTC	(Choy *et al.*, 2011)
CEN5	AAGAACTATGAATCTGTAAATGACT-GATTCAAT	CTTGCACTAAACAAGACTTTATACTAC-GTTTAG	P. Megee
ACT1	AATGGCGTGAGGTAGAGAGAAACC	ACAACGAATTGAGAGTTGCCCCAG	(Au *et al.*, 2008)
CON	ACTTTGCCTACTGCAGCACA	AAGCCGTTGCAATTCTTCAG	Basrai lab
CSE4	AACAACAATGGGTTAGTTCTGC	TTTCACTAGCCTTGCAAATGG	(Haase *et al.*, 2013)
Cdc7 f A Adapt T	AATTCCAGCTGACCACCATGACAAGCAAAACGAAGAATAT		This study
Cdc7 r w stop B Adapt T	GATCCCCGGGAATTGCCATGCTATTCAGATATTAGGAGAACATCCT		This study
Cdc7 r no stop GBP T	ACCAGCTGCACATCGGCCATTGATCCAGAACCTGATCCAGAACCTTCA-GATATTAGGAGAACATCCTTATC		This study

TABLE 2: List of PCR primers used in this investigation.

value of 100 for the wild-type strain. The frequency of chromosome segregation was determined by a colony color assay as described previously (Spencer *et al.*, 1990), in which the loss of a reporter CF results in red-colored sectors instead of a white-colored colony. Strains containing CF were grown to the logarithmic phase in medium selecting for the CF and plated on synthetic complete medium with limiting adenine at 25°C. About 1200 colonies were examined for each strain. The frequency of CF loss was calculated by counting the red-sectored colonies normalized to the total number of colonies and is shown as % chromosome loss.

In silico identification of Cdc7 target sites in Cse4 and mutagenesis

We performed sequence analysis to identify the predictive target sites of Cdc7 in Cse4 based on the DDK consensus target amino acid sequences as defined in previous studies (Cho *et al.*, 2006; Montagnoli *et al.*, 2006; Charych *et al.*, 2008; Sasanuma *et al.*, 2008; Wan *et al.*, 2008; Randell *et al.*, 2010; Hiraga *et al.*, 2014). We searched for consensus sites (S/T-D/E), which are defined by an acidic residue at the +1 position (Cho *et al.*, 2006; Montagnoli *et al.*, 2006; Charych *et al.*, 2008; Randell *et al.*, 2010; Hiraga *et al.*, 2014), as well as sites containing a negative charge at the +1 position created by a phosphoserine or phosphothreonine modified by another kinase (Sasanuma *et al.*, 2008; Wan *et al.*, 2008; Randell *et al.*, 2010). Mutant alleles of Cse4 were constructed synthetically by changing the predicted sites to alanine (A) or aspartic acid (D) by GeneScript (GeneScript). These synthetic mutant constructs were either integrated at the endogenous locus replacing the wild-type Cse4 with the mutant copy expressed from its native promoter (*cse4-4A* and *cse4-7A*) or cloned into *LEU2+ ARS4/CEN6* vector (pRS415, *cse4-4D*) to use in the complementation assay. The resultant constructs, namely, *vector::LEU2* (pRS415), *CSE4::LEU2* (pMB1725), and *cse4-4D::LEU2* (pMB2001) were then transformed into the *cse4Δ* strain carrying *CSE4::URA3* on a *CEN* plasmid (pRB199) to test for *CSE4* function by a plasmid shuffle assay.

SPI and microscopy

SPI screens were performed as previously described (Olafsson and Thorpe, 2015, 2018), which makes use of both the GFP-binding protein (Rothbauer *et al.*, 2008; Fridy *et al.*, 2014) and the GFP collection (Howson *et al.*, 2005). SPA is used to introduce plasmids into arrays of query yeast strains (Reid *et al.*, 2011). The resulting colonies were scanned with a desktop flatbed scanner (Epson V750 Pro, Seiko Epson Corporation, Japan). Colony sizes were determined and analyzed using ScreenMill and ScreenGarden software, which calculate log growth ratios (LGRs), a measure of the strength of the growth defect (Dittmar *et al.*, 2010; Klemm *et al.*, 2020). LGR values greater than 0.4 were considered to represent a growth defect in the screen, which represents at least a 45% drop in the number of yeast on the experimental condition versus the control. The cells were imaged with a Zeiss Axioimager Z2 microscope using a 63× 1.4 NA oil immersion lens, illuminated with a Zeiss Colibri LED light source (GFP = 470 nm, RFP = 590 nm). Bright-field contrast was enhanced using differential interference contrast prisms. Images were captured using a Flash 4.0 LT CMOS camera with 6.5 µm pixels binned 2 × 2 (Hamamatsu photonics, Japan). Images were processed with ImageJ and Icy softwares.

RNA extraction and reverse transcription (RT)-qPCR

Total RNA from the yeast cells was extracted using the Qiagen RNeasy kit and treated with DNase as per the manufacturer's instructions (Cat# 74106; Qiagen). DNase-treated RNA was reverse transcribed with the Access RT-PCR System (Promega Corporation, Madison, WI) in a 10-µl reaction using the primers for *CSE4* and *ACT1* (Table 2), and transcription levels were determined by real-time qPCR using 7500 Fast SYBR Green Master Mix (Applied Biosystems). RNA samples subjected to the RT step without reverse transcriptase enzyme were used as negative controls. The C_T values, representing the number of amplification cycles needed to cross the threshold fluorescence in the exponential region of amplification curve, were determined and used for the relative measurement of gene transcription.

ACKNOWLEDGMENTS

We are highly thankful to Sue Biggins, Georjana Barnes, and Inbal Gazy for strains and plasmids; Kathy McKinnon of the National Cancer Institute Vaccine Branch FACS Core for assistance with FACS; and the members of the Basrai laboratory for technical assistance and helpful discussions. P.K.M., W.C.A., J.R.E., L.B., and M.A.B. were supported by the Intramural Research Program of the National Cancer Institute, National Institutes of Health (NIH); M.W. was supported by The Van Andel Institute; R.A.S. was supported by NIH Grant R01GM35078; J.D.S. and K.B. were supported by NIH Grant R37 GM32238; and H.W. and P.H.T. were supported by the Queen Mary University of London.

REFERENCES

Asano S, Park JE, Sakchaisri K, Yu LR, Song S, Supavilai P, Veenstra TD, Lee KS (2005). Concerted mechanism of Swe1/Wee1 regulation by multiple kinases in budding yeast. EMBO J 24, 2194–2204.

Au WC, Crisp MJ, DeLuca SZ, Rando OJ, Basrai MA (2008). Altered dosage and mislocalization of histone H3 and Cse4p lead to chromosome loss in Saccharomyces cerevisiae. Genetics 179, 263–275.

Au WC, Dawson AR, Rawson DW, Taylor SB, Baker RE, Basrai MA (2013). A novel role of the N-terminus of budding yeast histone H3 variant Cse4 in ubiquitin-mediated proteolysis. Genetics 194, 513–518.

Au WC, Zhang T, Mishra PK, Eisenstatt JR, Walker RL, Ocampo J, Dawson A, Warren J, Costanzo M, Baryshnikova A, *et al.* (2020). Skp, cullin, F-box (SCF)-Met30 and SCF-Cdc4-mediated proteolysis of CENP-A prevents mislocalization of CENP-A for chromosomal stability in budding yeast. PLoS Genet 16, e1008597.

Berry LK, Olafsson G, Ledesma-Fernandez E, Thorpe PH (2016). Synthetic protein interactions reveal a functional map of the cell. eLife 5, e13053.

Boeckmann L, Takahashi Y, Au WC, Mishra PK, Choy JS, Dawson AR, Szeto MY, Waybright TJ, Heger C, McAndrew C, *et al.* (2013). Phosphorylation of centromeric histone H3 variant regulates chromosome segregation in Saccharomyces cerevisiae. Mol Biol Cell 24, 2034–2044.

Bruck I, Kaplan D (2009). Dbf4-Cdc7 phosphorylation of Mcm2 is required for cell growth. J Biol Chem 284, 28823–28831.

Burrack LS, Berman J (2012). Flexibility of centromere and kinetochore structures. Trends Genet 28, 204–212.

Calvert ME, Lannigan J (2010). Yeast cell cycle analysis: combining DNA staining with cell and nuclear morphology. Curr Protoc Cytom 53, 9.32.1–9.32.16.

Charych DH, Coyne M, Yabannavar A, Narberes J, Chow S, Wallroth M, Shafer C, Walter AO (2008). Inhibition of Cdc7/Dbf4 kinase activity affects specific phosphorylation sites on MCM2 in cancer cells. J Cell Biochem 104, 1075–1086.

Chen Y, Baker RE, Keith KC, Harris K, Stoler S, Fitzgerald-Hayes M (2000). The N terminus of the centromere H3-like protein Cse4p performs an essential function distinct from that of the histone fold domain. Mol Cell Biol 20, 7037–7048.

Cho WH, Lee YJ, Kong SI, Hurwitz J, Lee JK (2006). CDC7 kinase phosphorylates serine residues adjacent to acidic amino acids in the minichromosome maintenance 2 protein. Proc Natl Acad Sci USA 103, 11521–11526.

Choy JS, Acuna R, Au WC, Basrai MA (2011). A role for histone H4K16 hypoacetylation in Saccharomyces cerevisiae kinetochore function. Genetics 189, 11–21.

Ciftci-Yilmaz S, Au WC, Mishra PK, Eisenstatt JR, Chang J, Dawson AR, Zhu I, Rahman M, Bilke S, Costanzo M, *et al.* (2018). A genome-wide screen reveals a role for the HIR histone chaperone complex in preventing mislocalization of budding yeast CENP-A. Genetics 210, 203–218.

Clarke L, Carbon J (1980). Isolation of a yeast centromere and construction of functional small circular chromosomes. Nature 287, 504–509.

Dittmar JC, Reid RJ, Rothstein R (2010). ScreenMill: a freely available software suite for growth measurement, analysis and visualization of high-throughput screen data. BMC Bioinformatics 11, 353.

Eisenstatt JR, Boeckmann L, Au WC, Garcia V, Bursch L, Ocampo J, Costanzo M, Weinreich M, Sclafani RA, Baryshnikova A, *et al.* (2020). Dbf4-dependent kinase (DDK)-mediated proteolysis of CENP-A prevents mislocalization of CENP-A in saccharomyces cerevisiae. G3 (Bethesda) 10, 2057–2068.

Eisenstatt JR, Ohkuni K, Au WC, Preston O, Gliford L, Suva E, Costanzo M, Boone C, Basrai MA (2021). Reduced gene dosage of histone H4 prevents CENP-A mislocalization and chromosomal instability in saccharomyces cerevisiae. Genetics 218, iyab033.

Fridy PC, Li Y, Keegan S, Thompson MK, Nudelman I, Scheid JF, Oeffinger M, Nussenzweig MC, Fenyo D, Chait BT, Rout MP (2014). A robust pipeline for rapid production of versatile nanobody repertoires. Nat Methods 11, 1253–1260.

Fuller BG, Lampson MA, Foley EA, Rosasco-Nitcher S, Le KV, Tobelmann P, Brautigan DL, Stukenberg PT, Kapoor TM (2008). Midzone activation of aurora B in anaphase produces an intracellular phosphorylation gradient. Nature 453, 1132–1136.

Glowczewski L, Yang P, Kalashnikova T, Santisteban MS, Smith MM (2000). Histone-histone interactions and centromere function. Mol Cell Biol 20, 5700–5711.

Haase J, Mishra PK, Stephens A, Haggerty R, Quammen C, Taylor RM 2nd, Yeh E, Basrai MA, Bloom K (2013). A 3D map of the yeast kinetochore reveals the presence of core and accessory centromere-specific histone. Curr Biol 23, 1939–1944.

Hardy CF, Dryga O, Seematter S, Pahl PM, Sclafani RA (1997). mcm5/cdc46-bob1 bypasses the requirement for the S phase activator Cdc7p. Proc Natl Acad Sci USA 94, 3151–3155.

Henikoff S, Ahmad K, Platero JS, van Steensel B (2000). Heterochromatic deposition of centromeric histone H3-like proteins. Proc Natl Acad Sci USA 97, 716–721.

Hewawasam G, Shivaraju M, Mattingly M, Venkatesh S, Martin-Brown S, Florens L, Workman JL, Gerton JL (2010). Psh1 is an E3 ubiquitin ligase that targets the centromeric histone variant Cse4. Mol Cell 40, 444–454.

Hinshaw SM, Makrantoni V, Harrison SC, Marston AL (2017). The kinetochore receptor for the cohesin loading complex. Cell 171, 72–84 e13.

Hiraga S, Alvino GM, Chang F, Lian HY, Sridhar A, Kubota T, Brewer BJ, Weinreich M, Raghuraman MK, Donaldson AD (2014). Rif1 controls DNA replication by directing Protein Phosphatase 1 to reverse Cdc7-mediated phosphorylation of the MCM complex. Genes Dev 28, 372–383.

Hoang ML, Leon RP, Pessoa-Brandao L, Hunt S, Raghuraman MK, Fangman WL, Brewer BJ, Sclafani RA (2007). Structural changes in Mcm5 protein bypass Cdc7-Dbf4 function and reduce replication origin efficiency in Saccharomyces cerevisiae. Mol Cell Biol 27, 7594–7602.

Hoffmann G, Samel-Pommerencke A, Weber J, Cuomo A, Bonaldi T, Ehrenhofer-Murray AE (2018). A role for CENP-A/Cse4 phosphorylation on serine 33 in deposition at the centromere. FEMS Yeast Res 18.

Hollingsworth RE, Jr., Ostroff RM, Klein MB, Niswander LA, Sclafani RA (1992). Molecular genetic studies of the Cdc7 protein kinase and induced mutagenesis in yeast. Genetics 132, 53–62.

Howell RSM, Csikasz-Nagy A, Thorpe PH (2019). Synthetic physical interactions with the yeast centrosome. G3 (Bethesda) 9, 2183–2194.

Howson R, Huh WK, Ghaemmaghami S, Falvo JV, Bower K, Belle A, Dephoure N, Wykoff DD, Weissman JS, O'Shea EK (2005). Construction, verification and experimental use of two epitope-tagged collections of budding yeast strains. Comp Funct Genomics 6, 2–16.

Huh WK, Falvo JV, Gerke LC, Carroll AS, Howson RW, Weissman JS, O'Shea EK (2003). Global analysis of protein localization in budding yeast. Nature 425, 686–691.

Jackson AL, Pahl PM, Harrison K, Rosamond J, Sclafani RA (1993). Cell cycle regulation of the yeast Cdc7 protein kinase by association with the Dbf4 protein. Mol Cell Biol 13, 2899–2908.

Kastenmayer JP, Lee MS, Hong AL, Spencer FA, Basrai MA (2005). The C-terminal half of Saccharomyces cerevisiae Mad1p mediates spindle checkpoint function, chromosome transmission fidelity and CEN association. Genetics 170, 509–517.

Keith KC, Baker RE, Chen Y, Harris K, Stoler S, Fitzgerald-Hayes M (1999). Analysis of primary structural determinants that distinguish the centromere-specific function of histone variant Cse4p from histone H3. Mol Cell Biol 19, 6130–6139.

Klemm C, Thorpe PH, Olafsson G (2020). Cell-cycle phospho-regulation of the kinetochore. Curr Genet 67, 177–193.

Lampson MA, Cheeseman IM (2011). Sensing centromere tension: Aurora B and the regulation of kinetochore function. Trends Cell Biol 21, 133–140.

Lawrimore J, Bloom KS, Salmon ED (2011). Point centromeres contain more than a single centromere-specific Cse4 (CENP-A) nucleosome. J Cell Biol 195, 573–582.

Lei M, Kawasaki Y, Young MR, Kihara M, Sugino A, Tye BK (1997). Mcm2 is a target of regulation by Cdc7-Dbf4 during the initiation of DNA synthesis. Genes Dev 11, 3365–3374.

Livak KJ, Schmittgen TD (2001). Analysis of relative gene expression data using real-time quantitative PCR and the 2(-Delta Delta C(T)) method. Methods 25, 402–408.

Luger K, Rechsteiner TJ, Flaus AJ, Waye MM, Richmond TJ (1997). Characterization of nucleosome core particles containing histone proteins made in bacteria. J Mol Biol 272, 301–311.

Ma L, Ho K, Piggott N, Luo Z, Measday V (2012). Interactions between the kinetochore complex and the protein kinase A pathway in Saccharomyces cerevisiae. G3 (Bethesda) 2, 831–841.

Maddox PS, Bloom KS, Salmon ED (2000). The polarity and dynamics of microtubule assembly in the budding yeast Saccharomyces cerevisiae. Nat Cell Biol 2, 36–41.

Meluh PB, Yang P, Glowczewski L, Koshland D, Smith MM (1998). Cse4p is a component of the core centromere of Saccharomyces cerevisiae. Cell 94, 607–613.

Mishra PK, Au WC, Choy JS, Kuich PH, Baker RE, Foltz DR, Basrai MA (2011). Misregulation of Scm3p/HJURP causes chromosome instability in Saccharomyces cerevisiae and human cells. PLoS Genet 7, e1002303.

Mishra PK, Basrai MA (2019). Protein kinases in mitotic phosphorylation of budding yeast CENP-A. Curr Genet 65, 1325–1332.

Mishra PK, Baum M, Carbon J (2007). Centromere size and position in Candida albicans are evolutionarily conserved independent of DNA sequence heterogeneity. Mol Gen Genet 278, 455–465.
Mishra PK, Olafsson G, Boeckmann L, Westlake TJ, Jowhar ZM, Dittman LE, Baker RE, D'Amours D, Thorpe PH, Basrai MA (2019). Cell cycle-dependent association of polo kinase Cdc5 with CENP-A contributes to faithful chromosome segregation in budding yeast. Mol Biol Cell 30, 1020–1036.
Mishra PK, Thapa KS, Chen P, Wang S, Hazbun TR, Basrai MA (2018). Budding yeast CENP-A(Cse4) interacts with the N-terminus of Sgo1 and regulates its association with centromeric chromatin. Cell Cycle 17, 11–23.
Montagnoli A, Valsasina B, Brotherton D, Troiani S, Rainoldi S, Tenca P, Molinari A, Santocanale C (2006). Identification of Mcm2 phosphorylation sites by S-phase-regulating kinases. J Biol Chem 281, 10281–10290.
Musacchio A, Desai A (2017). A molecular view of kinetochore assembly and function. Biology (Basel) 6.
Natsume T, Muller CA, Katou Y, Retkute R, Gierlinski M, Araki H, Blow JJ, Shirahige K, Nieduszynski CA, Tanaka TU (2013). Kinetochores coordinate pericentromeric cohesion and early DNA replication by Cdc7-Dbf4 kinase recruitment. Mol Cell 50, 661–674.
Newlon CS (1988). Yeast chromosome replication and segregation. Microbiol Rev 52, 568–601.
Ohkuni K, Abdulle R, Kitagawa K (2014). Degradation of centromeric histone H3 variant Cse4 requires the Fpr3 peptidyl-prolyl Cis-Trans isomerase. Genetics 196, 1041–1045.
Ohkuni K, Levy-Myers R, Warren J, Au WC, Takahashi Y, Baker RE, Basrai MA (2018). N-terminal sumoylation of centromeric histone H3 variant Cse4 regulates its proteolysis to prevent mislocalization to non-centromeric chromatin. G3 (Bethesda) 8, 1215–1223.
Ohkuni K, Suva E, Au WC, Walker RL, Levy-Myers R, Meltzer PS, Baker RE, Basrai MA (2020). Deposition of centromeric histone H3 variant CENP-A/Cse4 into chromatin is facilitated by its C-terminal sumoylation. Genetics 214, 839–854.
Ohkuni K, Takahashi Y, Fulp A, Lawrimore J, Au WC, Pasupala N, Levy-Myers R, Warren J, Strunnikov A, Baker RE, *et al.* (2016). SUMO-Targeted Ubiquitin Ligase (STUbL) Slx5 regulates proteolysis of centromeric histone H3 variant Cse4 and prevents its mislocalization to euchromatin. Mol Biol Cell 27, 1500–1510.
Olafsson G, Thorpe PH (2015). Synthetic physical interactions map kinetochore regulators and regions sensitive to constitutive Cdc14 localization. Proc Natl Acad Sci USA 112, 10413–10418.
Olafsson G, Thorpe PH (2017). Rewiring the budding yeast proteome using synthetic physical interactions. Methods Mol Biol 1672, 599–612
Olafsson G, Thorpe PH (2018). Rewiring the budding yeast proteome using synthetic physical interactions. Methods Mol Biol 1672, 599–612.
Olafsson G, Thorpe PH (2020). Polo kinase recruitment via the constitutive centromere-associated network at the kinetochore elevates centromeric RNA. PLoS Genet 16, e1008990.
Ortiz J, Stemmann O, Rank S, Lechner J (1999). A putative protein complex consisting of Ctf19, Mcm21, and Okp1 represents a missing link in the budding yeast kinetochore. Genes Dev 13, 1140–1155.
Oshiro G, Owens JC, Shellman Y, Sclafani RA, Li JJ (1999). Cell cycle control of Cdc7p kinase activity through regulation of Dbf4p stability. Mol Cell Biol 19, 4888–4896.
Owens JC, Detweiler CS, Li JJ (1997). CDC45 is required in conjunction with CDC7/DBF4 to trigger the initiation of DNA replication. Proc Natl Acad Sci USA 94, 12521–12526.
Pearson CG, Yeh E, Gardner M, Odde D, Salmon ED, Bloom K (2004). Stable kinetochore-microtubule attachment constrains centromere positioning in metaphase. Curr Biol 14, 1962–1967.
Phizicky DV, Berchowitz LE, Berl SP (2018). Multiple kinases inhibit origin licensing and helicase activation to ensure reductive cell division during meiosis. eLife 7.
Randell JC, Fan A, Chan C, Francis LI, Heller RC, Galani K, Bell SP (2010). Mec1 is one of multiple kinases that prime the Mcm2-7 helicase for phosphorylation by Cdc7. Mol Cell 40, 353–363.
Ranjitkar P, Press MO, Yi X, Baker R, MacCoss MJ, Biggins S (2010). An E3 ubiquitin ligase prevents ectopic localization of the centromeric histone H3 variant via the centromere targeting domain. Mol Cell 40, 455–464.
Reid RJ, Gonzalez-Barrera S, Sunjevaric I, Alvaro D, Ciccone S, Wagner M, Rothstein R (2011). Selective ploidy ablation, a high-throughput plasmid transfer protocol, identifies new genes affecting topoisomerase I-induced DNA damage. Genome Res 21, 477–486.
Robellet X, Thattikota Y, Wang F, Wee TL, Pascariu M, Shankar S, Bonneil E, Brown CM, D'Amours D (2015). A high-sensitivity phospho-switch triggered by Cdk1 governs chromosome morphogenesis during cell division. Genes Dev 29, 426–439.
Rossbach D, Bryan DS, Hesselberth JR, Sclafani R (2017). Localization of Cdc7 protein kinase during DNA replication in saccharomyces cerevisiae. G3 (Bethesda) 7, 3757–3774.
Rothbauer U, Zolghadr K, Muyldermans S, Schepers A, Cardoso MC, Leonhardt H (2008). A versatile nanotrap for biochemical and functional studies with fluorescent fusion proteins. Mol Cell Proteomics 7, 282–289.
Rothbauer U, Zolghadr K, Tillib S, Nowak D, Schermelleh L, Gahl A, Backmann N, Conrath K, Muyldermans S, Cardoso MC, Leonhardt H (2006). Targeting and tracing antigens in live cells with fluorescent nanobodies. Nat Methods 3, 887–889.
Samel A, Cuomo A, Bonaldi T, Ehrenhofer-Murray AE (2012). Methylation of CenH3 arginine 37 regulates kinetochore integrity and chromosome segregation. Proc Natl Acad Sci USA 109, 9029–9034.
Santaguida S, Amon A (2015). Short- and long-term effects of chromosome mis-segregation and aneuploidy. Nat Rev Mol Cell Biol 16, 473–485.
Sasanuma H, Hirota K, Fukuda T, Kakusho N, Kugou K, Kawasaki Y, Shibata T, Masai H, Ohta K (2008). Cdc7-dependent phosphorylation of Mer2 facilitates initiation of yeast meiotic recombination. Genes Dev 22, 398–410.
Schneider CA, Rasband WS, Eliceiri KW (2012). NIH Image to ImageJ: 25 years of image analysis. Nat Methods 9, 671–675.
Sclafani RA, Tecklenburg M, Pierce A (2002). The mcm5-bob1 bypass of Cdc7p/Dbf4p in DNA replication depends on both Cdk1-independent and Cdk1-dependent steps in Saccharomyces cerevisiae. Genetics 161, 47–57.
Sikorski RS, Hieter P (1989). A system of shuttle vectors and yeast host strains designed for efficient manipulation of DNA in Saccharomyces cerevisiae. Genetics 122, 19–27.
Singh VP, Gerton JL (2015). Cohesin and human disease: lessons from mouse models. Curr Opin Cell Biol 37, 9–17.
Smith MM, Yang P, Santisteban MS, Boone PW, Goldstein AT, Megee PC (1996). A novel histone H4 mutant defective in nuclear division and mitotic chromosome transmission. Mol Cell Biol 16, 1017–1026.
Spencer F, Gerring SL, Connelly C, Hieter P (1990). Mitotic chromosome transmission fidelity mutants in Saccharomyces cerevisiae. Genetics 124, 237–249.
St-Pierre J, Douziech M, Bazile F, Pascariu M, Bonneil E, Sauve V, Ratsima H, D'Amours D (2009). Polo kinase regulates mitotic chromosome condensation by hyperactivation of condensin DNA supercoiling activity. Mol Cell 34, 416–426.
Stoler S, Keith KC, Curnick KE, Fitzgerald-Hayes M (1995). A mutation in CSE4, an essential gene encoding a novel chromatin-associated protein in yeast, causes chromosome nondisjunction and cell cycle arrest at mitosis. Genes Dev 9, 573–586.
Sullivan KF, Hechenberger M, Masri K (1994). Human CENP-A contains a histone H3 related histone fold domain that is required for targeting to the centromere. J Cell Biol 127, 581–592.
Takahashi K, Chen ES, Yanagida M (2000). Requirement of Mis6 centromere connector for localizing a CENP-A-like protein in fission yeast. Science 288, 2215–2219.
Verdaasdonk JS, Bloom K (2011). Centromeres: unique chromatin structures that drive chromosome segregation. Nat Rev Mol Cell Biol 12, 320–332.
Wan L, Niu H, Futcher B, Zhang C, Shokat KM, Boulton SJ, Hollingsworth NM (2008). Cdc28-Clb5 (CDK-S) and Cdc7-Dbf4 (DDK) collaborate to initiate meiotic recombination in yeast. Genes Dev 22, 386–397.
Weinreich M, Stillman B (1999). Cdc7p-Dbf4p kinase binds to chromatin during S phase and is regulated by both the APC and the RAD53 checkpoint pathway. EMBO J 18, 5334–5346.
Wisniewski J, Hajj B, Chen J, Mizuguchi G, Xiao H, Wei D, Dahan M, Wu C (2014). Imaging the fate of histone Cse4 reveals de novo replacement in S phase and subsequent stable residence at centromeres. eLife 3, e02203.
Wu KZ, Wang GN, Fitzgerald J, Quachthithu H, Rainey MD, Cattaneo A, Bachi A, Santocanale C (2016). DDK dependent regulation of TOP2A at centromeres revealed by a chemical genetics approach. Nucleic Acids Res 44, 8786–8798.
Zou L, Stillman B (2000). Assembly of a complex containing Cdc45p, replication protein A, and Mcm2p at replication origins controlled by S-phase cyclin-dependent kinases and Cdc7p-Dbf4p kinase. Mol Cell Biol 20, 3086–3096.